Laminar Burning Velocity Measurement of Hydrous Methanol at Elevated Temperatures and Pressures

Kun Liang [a*], Richard Stone [b]

[a] *Department of Engineering and Design, University of Sussex, Brighton BN1 9QT, UK*

[b] *Department of Engineering Science, University of Oxford, Oxford OX1 3PJ, UK*

* Corresponding author. Tel: +44 1273 678573. Email address: kun.liang@sussex.ac.uk (K. Liang)

Abstract

Methanol is an important renewable energy source that absorbs water easily. The water can be present inadvertently or as a result of the manufacturing process. Although adding water into methanol will further improve the anti-knock rating for spark ignition engines, the burning velocity, flame stability and the flammability range will be reduced. The laminar burning velocity of methanol containing up to 40% water in volume has been measured for a wide range of temperature (350-450 K), pressures (1-4 bar) and equivalence ratio (0.7-1.4) using a constant volume vessel and a schlieren imaging system. The experimental data using the pressure rise data (but excluding cellularity) have been fitted to a correlation with twelve coefficients. Results showed a decrease in burning velocity with pressure and an increase with temperature. Water as a diluent led to reduction of the burning velocity. The correlated burning velocity data for methanol are in good agreement with published data. The cellularity occurred earlier as the initial mixture became rich, while a higher water fraction delayed the onset of cellularity.

Keywords: Laminar burning velocity, Constant volume, Hydrous methanol, Cellularity

1. Introduction

Methanol is an alternative fuel for internal combustion engines, which has gained popularity due to its lower cost compared to ethanol. Methanol can be produced from a wide range of renewable sources such as gasification of wood, agricultural by-products and urban waste, in addition to using fossil fuels based feedstock (coal and natural gas) **[1]**. Widespread production from renewable sources has a potential to offer methanol at a low cost and with benefits to the environment. Due to its high octane rating, high latent heat and low combustion temperatures, the power and efficiency are significantly higher for methanol (and ethanol) compared to gasoline. This is especially true for highly pressure-charged engines, where aggressive downsizing is possible using these alcohols **[2]**.

Methanol is hygroscopic, meaning purified methanol by distillation will absorb water vapour directly from the atmosphere. Although adding water will improve the anti-knock rating, it dilutes the calorific value of the methanol, and may cause phase separation of methanol-gasoline blends. The water diluent will reduce the burning velocity, the flame stability and the flammability range, all of which would lead to adverse effects on the combustion system performance. Pearson et al. **[3]** concluded that the blends with only gasoline and ethanol have the highest water tolerance, which decreases monotonically as the ethanol was displaced by increasing amounts of methanol.

The laminar burning velocity is among the most fundamental properties characterizing the combustion of homogeneous fuel-air mixtures. It can also be used to validate the chemical-kinetic mechanism and estimate the turbulent burning velocity. The laminar burning velocity depends on the initial pressure, mixture temperature and equivalence ratio of the unburned mixture.

The laminar burning velocities of methanol have been conducted by many researchers using different experimental approaches. Saeed and Stone **[4]** used a multi-zone thermodynamic model to determine the temperature distribution within the burned gas and the relationship between the pressure rise and the mass fraction burned in a constant-volume vessel. They used a constant volume bomb to measure the laminar burning velocity of methanol at elevated temperature and pressures. The onset of cellular flame was estimated by looking at the calculated burning velocity. Results show that the variation of temperature exponent with equivalence ratio was linear. Metghalchi and Keck **[5]** had previously used a constant volume bomb to measure the laminar burning velocity of methanol. Gulder **[6]** also adopted a constant volume bomb for measuring burning velocity of methanol at atmospheric pressure. Neither of these two studies considered the onset of cellularity when calculating the laminar burning velocity. Liao et al. **[7, 8]** and Zhang et al. **[9, 10]** used a constant volume bomb and a schilieren image system with high speed camera to determine the unstretched laminar burning velocity of methanol at elevated temperatures and pressures.

Steady flame techniques have also been widely used, but are normally limited to conditions close to ambient. Davies and Law **[11]** and Egolfopoulos et al. **[12]** adopted a counterflow flame configuration to measure the laminar flame speed of methanol. Gibbs and Calcote **[13]** used a Bunsen burner and a camera to study the burning velocity of methanol. Vancoillie et al. **[14]** used a perforated plate burner to obtain measurements of the laminar burning velocity of methanol at unburned mixture temperature of 298-353K and atmospheric pressure. The heat flux method was used to determine burning velocities under conditions when the net heat loss from the flame to the burner is zero. Sileghem et al. **[15]** used a similar method to study the temperature dependency at atmospheric pressure in order to validate the reaction mechanism. However, experiments with higher pressures have not been reported.

Recently Beeckmann et al. **[16]** measured the laminar burning velocity of methanol at an unburned temperature of 373 K and a pressure of 10 bar in a spherical combustion vessel using schlieren optical system. The sensitivity analysis for methanol/air flames suggested further investigation of the pressure dependent reactions. Most recently, Katoch et al. **[17]** used an externally heated meso-scale diverging channel technique to measure the laminar burning velocity of methanol. Experiments were carried out for unburned mixture temperature of 350-650 K at atmospheric pressure. Good agreement was observed at 300 K with published experimental data.

The constant volume combustion method is capable of exploiting the increase in pressure and the resulting increase in unburned gas temperature. Values of the burning velocity can be calculated for multiple temperatures and pressures from a single experiment as the pressure rise causes an isentropic temperature increase in the unburned gas. Therefore, the burning velocity can be determined from the pressure trace inside the combustion bomb by assuming a smooth spherical flame front and an appropriate combustion model **[18]**. Although there are many published data for methanol, the burning velocity of hydrous methanol has not been

investigated so far. The objective of the present work is to extend the constant volume method and schlieren image system to measure the laminar burning velocity of methanol/water blends at higher unburned mixture temperatures and pressures. W0 is pure methanol. W20 and W40 mean water volume fractions of 20% and 40%, respectively.

2. Experimental Apparatus

The combustion bomb for this work is the same as described elsewhere **[18, 19, 20]**. The constant volume bomb shown in Fig. 1 is a stainless steel spherical vessel with a diameter of 160 mm rated to 34 bar. The combustion vessel was enclosed by a temperature controlled fan oven, which can increase the initial temperature up to 450 K. Two electrodes formed a spark gap at the centre of the vessel. An automotive inductive ignition system was used. The compressed intake air was controlled by a mass flow controller and heated before going into an injection block, which was also heated to ensure evaporation of the liquid fuel. The liquid fuel volume and injection speed of the syringe actuator were controlled by a syringe controller. A Kistler 710A piezo-electric pressure transducer was employed to measure the pressure rise during combustion. Three piezo-resistive pressure transducers with different ranges were also used for measuring pressures during evacuation and mixture preparation. An exposed junction K-type thermocouple was fitted into the vessel to measure the temperature during mixture preparation. A LabVIEW programme has been written to display the pressure and temperature during mixture preparation and record the pressure data after ignition. The sampling rate during combustion was 10 kHz. A heated wideband lambda sensor was located in the exhaust line for the combustion bomb, in order to monitor the air fuel ratio of the burned products.

The pressure vessel had a pair of windows with 40 mm diameter along the optical axis (see Fig. 1) to allow a schlieren imaging system, which was adopted to track early flame growth and help detect the cellularity. The schlieren images were recorded using a Photron 1024 PCI high speed camera with a 512×512 pixel resolution, allowing a frame rate of 3000 frame per second (fps).

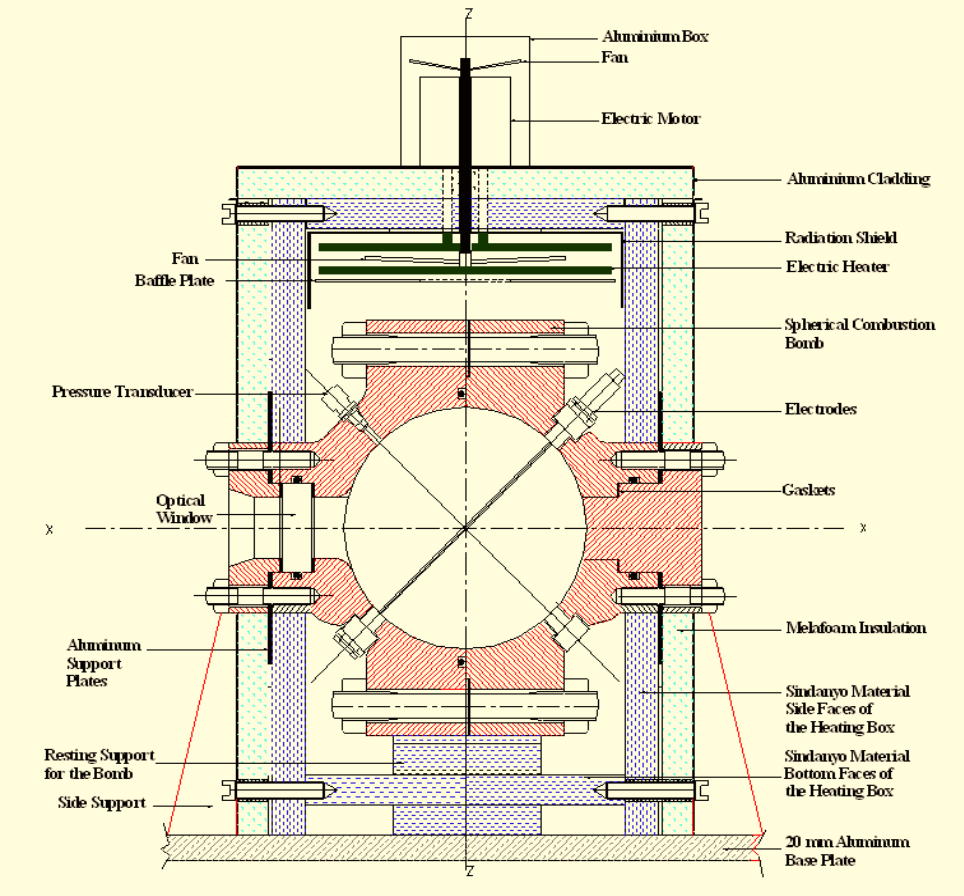

Fig. 1 Schematic of the constant volume combustion bomb with optical windows (only one shown) for schlieren imaging system

The experimental procedure was similar to **[18, 19, 20]** apart from using a digital balance with 0.1 mg resolution to measure the mass of liquid fuel injected. The fuel was injected using a Hamilton precision syringe with a motorised actuator, and the mass was measured before and after injection. For each test, the volume of fuel required was determined by the initial temperature, target pressure and equivalence ratio. The target pressure was set to be higher than the pressure at the start of combustion. After injection of fuel, the bomb pressure was raised by increasing the air flow rate up to the target pressure that had been calculated on the basis of the mass of fuel that had been injected. The waiting time was 5 mins before reducing the bomb pressure down to the mixture pressure for ignition.

3. Laminar Burning Velocity

Fig. 2 shows the schematic of the calculation and correlation of the laminar burning velocity in MATLAB. For every single experiment, the pressure trace p(t) during combustion recorded by LabVIEW (Fig. 2a) was used to calculate the burning velocity according to the equation given by Lewis and Von Elbe **[21]**:

$$S_u = \frac{dr_i}{dt}\left(\frac{r_i}{r_b}\right)^2\left(\frac{p}{p_i}\right)^{\frac{1}{\gamma u}} \quad (1)$$

where r_i is the initial radius of the current mass fraction burned prior to combustion, r_b is the flame radius, γ_u is the ratio of specific heats of the unburned mixture, and p_i is the initial pressure.

The initial radius r_i depends on the mass fraction burned as follow:

$$r_i = \sqrt[3]{xR^3} \tag{2}$$

where *x* is the mass fraction burned and *R* is the radius of the pressure vessel.

A multi-zone combustion model **[22]** named BOMB Program in Fig. 2 was then used to define the relationship between *p* and *x*. The BOMB program solved the composition for the equilibrium of ten major combustion products for each zone, as well as the conservation equations for energy and mass; it assumed negligible flame front thickness. The basic thermochemical properties for the fuel and the experimental conditions (initial temperature, pressure and equivalence ratio) were the inputs into the BOMB program. This model was also used to relate the pressure to flame radius, unburned gas temperature and temperature distribution within the burned gases for each experiment. The results of the BOMB program were used to calculate the burning velocity for all conditions of unburned gas temperature and pressure during the combustion (see blue curve in Fig. 2b).

The images from the schlieren optical system were processed by a MATLAB routine, which used an edge detection algorithm. The rapid segmentation caused by cellularity resulted in a rapid and prolonged increase in the number of edges, which can be detected. This then allowed the detection of the onset of cellularity for each experiment so that the burning velocity data affected by cellularity can be excluded. Fig. 2b gives an example of how the flame front propagated. The onset of cellularity means that calculating the laminar burning velocity using the pressure record is no longer possible as the smooth flame front assumption is invalid. The red vertical dotted line identifies the onset of cellularity. The flame speed can also be deduced from the schlieren image of flame front propagation. Spherically expanding flames are initially highly stretched, so unstretched flame speed data were obtained by extrapolating back to zero stretch. The details of the schlieren image system are described in **[20]**.

The desired range of burning velocity data from each experiment for the correlation ignored the noisy early burn stage and excluded any data after the onset of cellularity. The selected data from all the experiments and the images formed the full data set for the correlation. A least squares minimisation algorithm was used to determine the correlation coefficients. The correlation gives burning velocity S_u as a function of pressure *P*, temperature *T* and equivalence ratio $\emptyset$ as follow:

$$S_u = \left[S_{u,0} + S_{u,1}(\phi - 1) + S_{u,2}(\phi - 1)^2 + S_{u,3}(\phi - 1)^3 + S_{u,4}(\phi - 1)^4\right] \times T^{\alpha} P^{\beta} \tag{3}$$

where $S_{u,i}$ is the polynomial coefficients. The temperature and pressure of the unburned gas are normalised by 298 K and 1 bar.

$$T = \frac{T_u}{298} \tag{4}$$

$$P = \frac{P_u}{1} \tag{5}$$

The exponents α and β for temperature and pressure respectively are also expressed as functions of the equivalence ratio $\emptyset$:

$$\alpha = \alpha_0 + (\emptyset - 1)\alpha_1 \tag{6}$$

$$\beta = \beta_0 + (\emptyset - 1)\beta_1 \quad (7)$$

Fig. 2c shows an example of the correlated burning velocity (in blue) in comparison with experimental data (in red). The final correlation can be plotted for any temperature, pressure and equivalence ratio as can be seen in Fig. 2d.

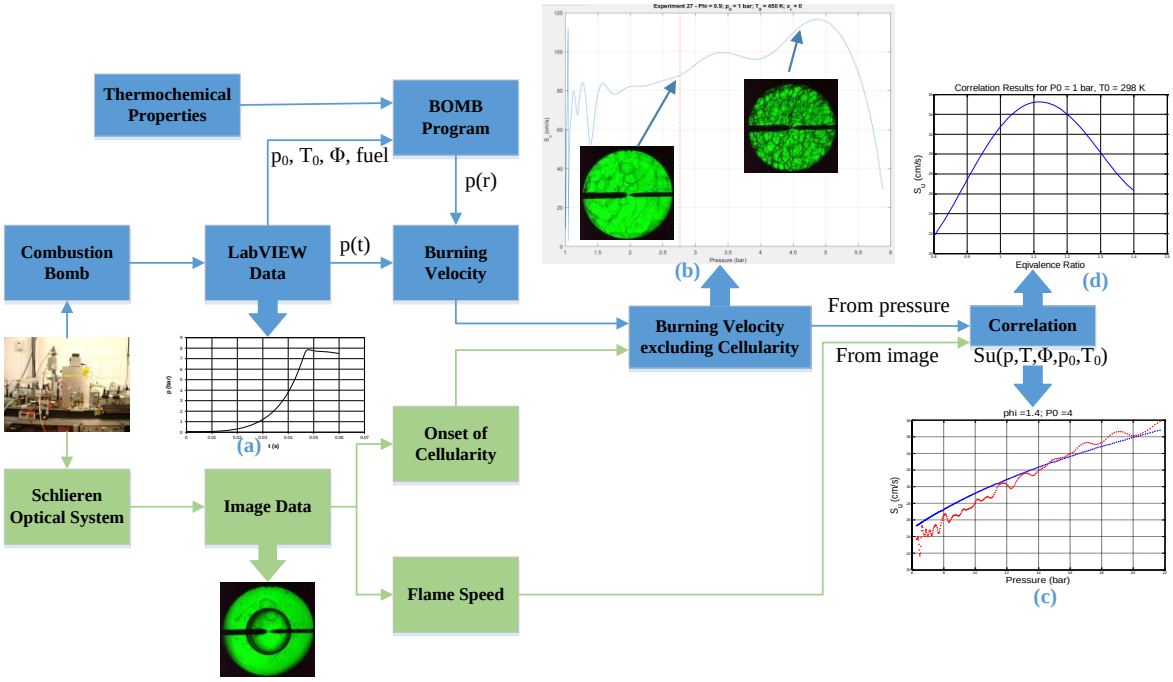

Fig. 2 Schematic of the combustion bomb data analysis combining data from both pressure trace and schlieren image records. Blue boxes and arrows are for data flow from pressure trace (LabVIEW data); green boxes and arrows are for data flow from schlieren images. 2(a) shows the pressure rise record, 2(b) shows the derived value of the burning velocity plotted against pressure rise, along with images showing cellularity, 2(c) shows the fit form the overall correlation to an individual experiments and 2(d) illustrates the output form the correlation.

As has been pointed out by Hinton and Stone **[18]**, when there is sufficient pressure rise for the pressure record to be used in calculating the burning velocity; the stretch rate is sufficiently small such that it can be ignored. As the flame propagates outwardly, the flame stretch rate decreases and flame propagation speed increases.

4. Results and Discussions

4.1 Correlation Coefficients

A total of 144 experiments were conducted over a range of initial temperatures (380 K and 450 K), pressures (1 bar, 2 bar and 4 bar) and equivalence ratios (0.7 – 1.4) for 3 methanol/water blends (W0, W20, and W40). It should be noted that for some experiments of W20 and W40, at 350 K and equivalence ratio of 0.7 (very lean fuel-air mixture), there was no combustion. Table 1 shows the minimum and maximum values of the data sets that were used for the correlation fitting. As expected, maximum unburned gas temperature, pressure and burning velocity decreases with increasing water fraction.

Table 1 Minimum and maximum values for methanol/water data sets (W20 means 20% water by volume)

		W0		W20		W40	
	Units	Min	Max	Min	Max	Min	Max
Initial temperature, T_0	K	380	450	380	450	380	450
Initial pressure, P_0	bar	1	4	1	4	1	4
Equivalence ratio, $\emptyset$		0.7	1.4	0.7	1.4	0.7	1.4
Unburned gas pressure, P_u	bar	1.2	23.6	1.2	21.1	1.1	20.2
Unburned gas temperature, T_u	K	381.6	671.1	383.1	663.1	389.7	642.5
Burning velocity, S_μ	cm/s	15.5	130.8	6.6	85.6	5.1	73.1
Flame speed, S_f	cm/s	25.1	449.5	15.2	308.4	12.5	182
Stretch rate, α	/s	6.4	338.2	2.1	246.3	0.9	102.9
Flame radius, r_b	mm	18.7	77.9	22.7	78.8	30.1	79.5

The correlation coefficients obtained from the fitting process according to Equation 3 are given in Table 2. It can be seen that pure methanol (W0) has the highest $S_{\mu,0}$ indicating highest burning velocity among three fuels when $\emptyset$ = 1 (stoichiometric), P_u = 1 bar and T_u = 298 K. The range of conditions over which this correlation can be reliably correlated is limited by the spread of data that was used to establish the correlation. Therefore, the correlation results could not be relied upon to provide accurate values of laminar burning velocity for low temperatures and pressures (below around 330 K and 1 bar).

Table 2 Coefficients to give burning velocity for three fuels from Equation 3

	$S_{\mu,0}$	$S_{\mu,1}$	$S_{\mu,2}$	$S_{\mu,3}$	$S_{\mu,4}$	α_0	α_1	β_0	β_1
W0	32.2252	20.1917	-167.1270	-63.5209	644.2650	2.4659	0.7395	-0.2971	-0.4397
W20	18.3261	12.6511	-87.8459	20.9271	176.5145	2.7645	0.7020	-0.4227	-0.0786
W40	17.8310	23.2869	-66.7418	-150.0042	298.2621	1.7202	-0.3379	-0.2929	0.2791

4.2 Laminar Burning Velocity Correlation Results

Fig. 3 shows the correlation for the laminar burning velocities at elevated temperatures for stoichiometric methanol water blends at P_u = 2 bar. Increasing the temperature of the mixture results in a faster burning velocity as expected. Methanol is known to have a higher stoichiometric laminar burning velocity at ambient conditions than isooctane and ethanol **[6]**. However, when blended with water, the burning velocity reduces. The higher fraction of water led to slower burning. The difference between pure methanol and hydrous methanol increases dramatically with temperature. When P_u = 2 bar and T_u = 400 K, the laminar burning velocities for W0, W20 and W40 are 54.2 cm/s, 30.8 cm/s, 24.2 cm/s respectively. The difference between W0 and W20 are much smaller than between W0 and W40. This is due to the temperature exponent (α_0, and α_1) being very close to each other for W0 and W20.

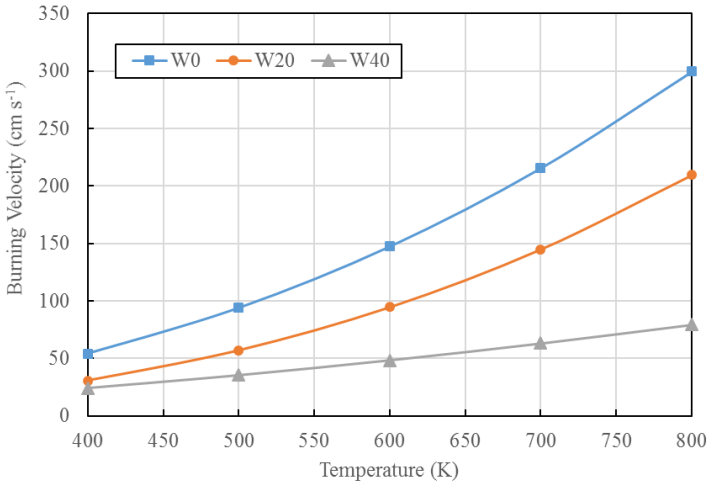

Fig. 3 Correlations for the laminar burning velocity against temperature evaluated at 2 bar for stoichiometric mixtures of methanol with different water fractions

Fig. 4 shows the correlated burning velocities as a function of equivalence ratio for 3 fuels at T_u = 450 K and P_u = 2 bar. The influence of water on the laminar burning velocity can be further demonstrated. As water as a diluent does not participate in the chemical reaction but changes the specific heat capacity of the mixture and reduces the flame temperature during combustion, the burning velocity is reduced. The peak burning velocity is observed at slightly rich mixtures. The burning velocity for pure methanol (W0) peaks at an equivalence ratio close to 1.1 which agrees with most of the available data in the literature. A detailed comparison with other literature results is given in Section 4.3. Fig. 4 also shows a trend for the peak burning velocity to shift away from stoichiometric as the fraction of water is increased.

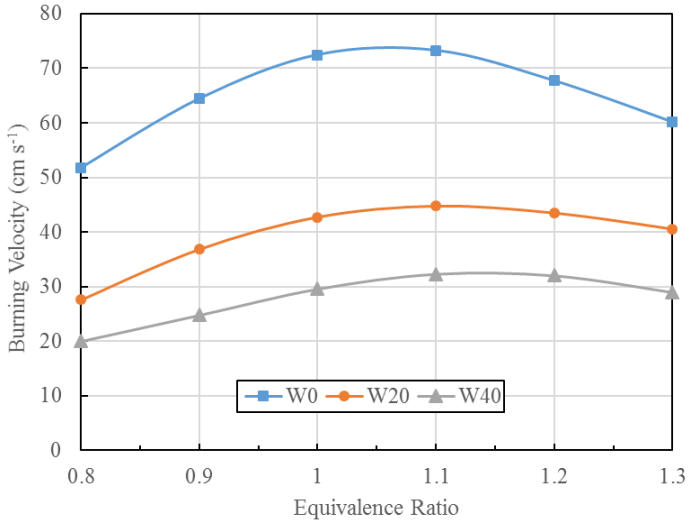

Fig. 4 Correlations for the laminar burning velocity of methanol with different water fractions at T_u = 450 K and P_u = 2 bar

Fig. 5 shows the comparison of correlated burning velocities for the 3 fuels at different pressure at T_u = 400 K. As expected, increasing the pressure results in a lower laminar burning velocity. The peak burning velocity for W40 is lower than the minimum for W0.

This indicates that adding 40% water (by volume) would make the methanol unsuitable for a combustion engine. The peak burning velocities for W0, W20 and W40 are 69 cm/s, 43 cm/s, 32 cm/s respectively. The effect of pressure on the burning velocity depends on the pressure exponent (β_0, β_1) in Table 1.

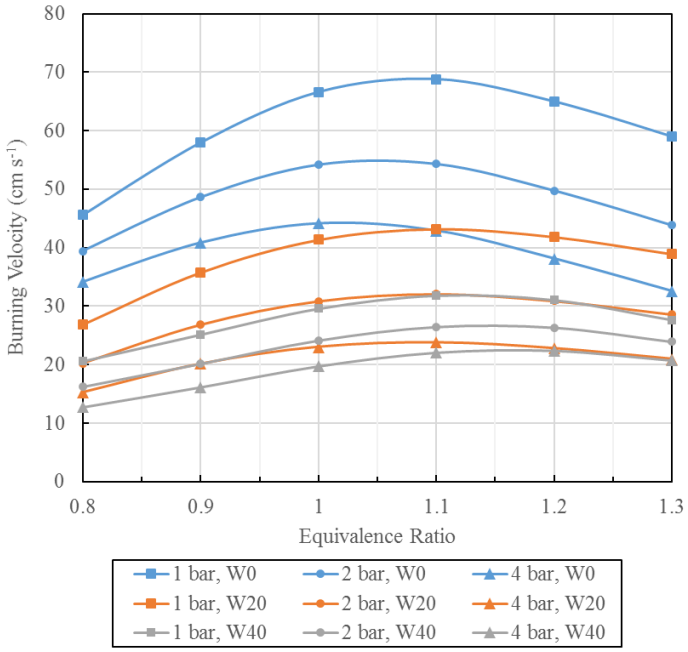

Fig. 5 Comparison of the correlations for the laminar burning velocity of methanol with different water fractions at T_u = 400 K

4.3 Comparison of Methanol Results with Other Data

The laminar burning velocity for pure methanol W0 for this work was extrapolated down to 300 K (ambient temperature) as this is a condition which has been frequently reported by many researchers. Fig. 6 compares the present results with available experimental data in the literature. It is interesting to see that the extrapolated values are in good agreement with the experimental results of Metghalchi and Keck **[5]**, particularly at lower equivalence ratios. Both experiments used constant volume combustion bomb and cellular data in **[5]** probably causes the higher data on the richer side. For leaner mixtures, Gibbs and Calcote **[13]** reported the highest values but conical flame measurements are now not accurate. On the richer side, Saeed and Stone **[4]** reported the highest values and the present values are the lowest. The explanation for this is very early cellularity was observed with rich mixtures using the schlieren imaging system prior to it being noticeable in the data derived from the pressure rise. It should be noted that most of reported measurements in the literature are for an ambient temperature but in this work the lowest initial temperature is 380 K. This indicates that extrapolation down to 300 K may not be very reliable for comparison. Among the available data, Metghalchi and Keck **[5],** Liao et al. **[7]**, Saeed and Stone **[4]** all present work using a constant volume vessel for measurements. Therefore, it is worth comparing results from these 4 measurements at higher temperatures and pressures. When calculating the laminar burning velocity, ignoring cellularity would perhaps lead to over prediction of the value since the presence of cellular structures in a flame front causes increase in burning velocity due to increased surface area.

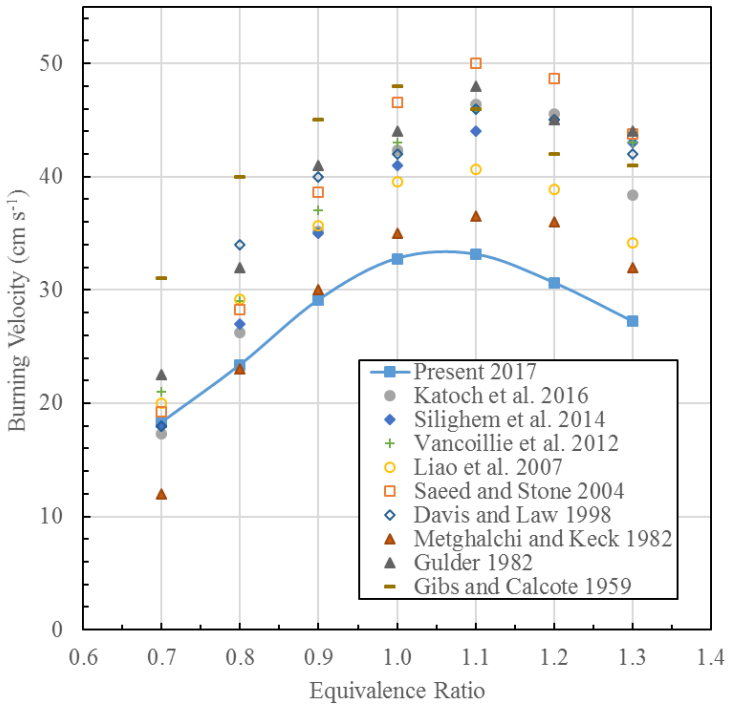

Fig. 6 Comparison of the laminar burning velocity of methanol at ambient temperature (300 K) and atmospheric pressure (1 bar) with available experimental data; the data from the current work has required downwards extrapolation so must be treated with caution

Fig. 7 compares the correlated burning velocity of methanol for the present work with 3 other available experimental studies using a constant volume vessel at T_u = 400 K and P_u = 2 bar. As Liao et al. **[7]** only measured the burning velocity at atmospheric pressure, a pressure exponents were applied to their correlation. It can be seen that the present data agrees very well with Liao et al. **[7]** across the equivalence ratios. When the mixture is lean, the present data are in very good agreement with all other 3 results. As the mixture becomes rich, Metghalchi and Keck **[5]** and Saeed and Stone **[4]** show consistent and higher values. This is probably because Metghalchi and Keck **[5]** have over predicted the burning velocity without detecting the cellular flame. Although Saeed and Stone **[4]** used a similar experimental apparatus and reported cellularity by looking at the burning velocity variation (no schlieren system was used at the time), the cellularity was found to occur much earlier when analysing the flame images from the schlieren system compared with the pressure rise data. This means that Saeed and Stone **[4]** could also have over predicted the burning velocity. A discussion on the onset of cellularity is given in Section 4.4.

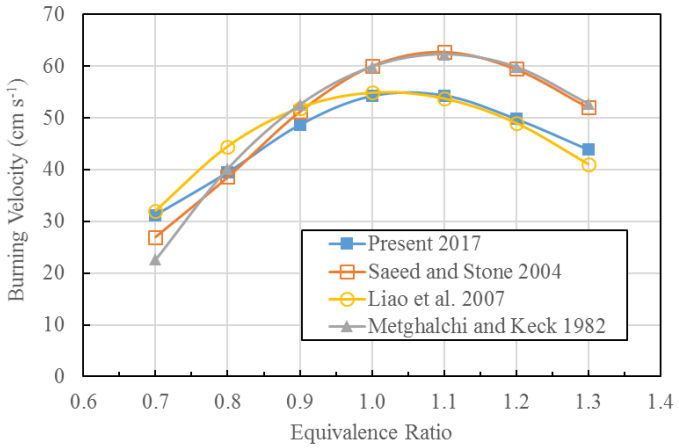

Fig. 7 Comparison of the laminar burning velocity of methanol at T_u = 400 K and P_u = 2 bar with available experimental data (using constant volume vessel); there is good agreement for lean mixture where there is less influence from cellularity

4.4 Cellularity

Fig. 8 shows the pressure at the onset of cellularity for W0, W20 and W40, which are plotted here for all tested initial temperatures, pressures and equivalence ratios. Other criteria were investigated at the onset of cellularity, and it appears that the pressure is the most significant indicator. In contrast, initial temperature has negligible effect on the value of pressure at the onset of cellularity across the equivalence ratios. In general, cellularity occurs earlier as the initial pressure increases. It can also be seen that for most conditions (initial pressure and temperature) when the initial mixture is lean or stoichiometric, the pressure at the onset of cellularity drops dramatically as the equivalence ratio increases. When the mixture becomes rich, the pressure at the onset of cellularity appears to be more stable. For the case of W0 at 380 K and 4 bar, as the mixture becomes rich, the cellularity occurs around 4.2 bar, which is at a very early stage of combustion. It is worth mentioning that for the case of W20 and W40, when the mixture is very lean, no cellularity in the flame was found.

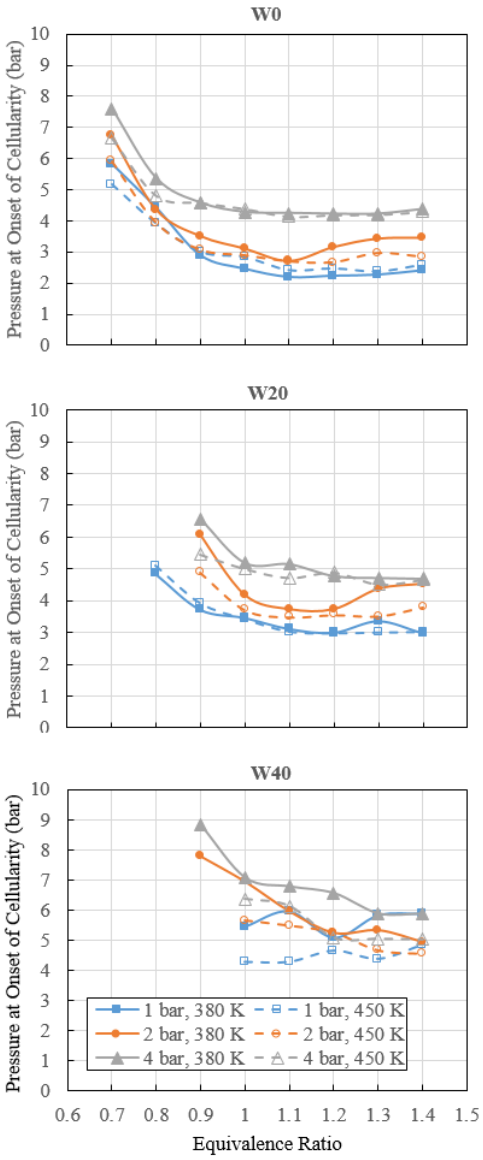

Fig. 8 Pressure at the onset of cellularity plotted against equivalence ratio for methanol with different water fractions at different initial temperatures and pressures; note that for the 4 bar initial pressure data the onset of cellularity was essentially immediate for the rich mixtures of W0 and W20

Fig. 9 compares the pressure at the onset of cellularity for methanol with different water fractions at T_u = 380 K and P_u = 4 bar, and as before, for the 4 bar data the onset of cellularity was essentially immediate for the rich mixtures of W0 and W20. It is clear that increasing the water fraction delays the onset of cellularity across the equivalence ratios since the cellularity is seen to occur at higher pressures as water fraction rises. The pressure at the onset of cellularity is higher for the lean mixtures.

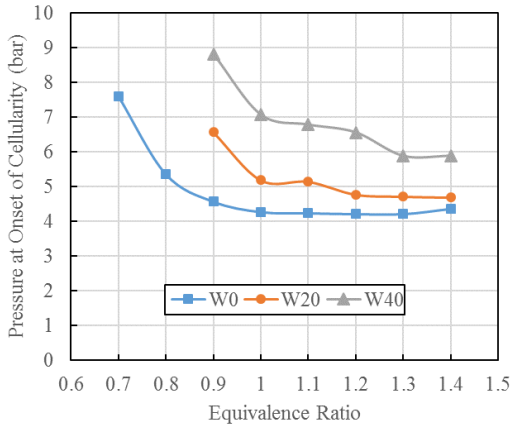

Fig. 9 Comparison of the pressure at onset of cellularity plotted against equivalence ratio for different water fractions at T_u = 380 K and P_u = 4 bar

5. Conclusions

The laminar burning velocity of methanol containing water with different volume fractions has been measured by using a constant volume combustion bomb and a schlieren imaging system. Experiments over a wide range of initial temperatures, pressures and equivalence ratios have been conducted to generate an overall data set for the final correlation. Cellularity was detected so that the burning velocity data after the onset of cellularity can be excluded so as to avoid over prediction. The data reported here has the expected trends:

(1) Higher pressures lead to a lower laminar burning velocity. Increasing the temperature will raise the burning velocity. The peak burning velocity appears to be close to equivalence ratio of 1.1 for pure methanol (W0), which agrees with most of the available results in the literature.

(2) Increasing the fraction of water tends to decrease the burning velocity of methanol sharply. Methanol containing 40% water in volume (W40) appears to burn significantly more slowly. Adding more water will shift the equivalence ratio of the peak burning velocity.

(3) Comparisons of methanol with published data are limited, since most experiments are conducted at close to ambient conditions. A more meaningful comparison was made with 3 experimental studies, all of which used the constant volume vessel. A very close agreement has been observed, particularly for lean combustion. It is also concluded that for rich mixtures, the present data are more accurate because the detection of cellularity occurs earlier when using a schlieren imaging system than by looking at the burning velocity variation.

(4) The initial temperature has negligible influence on the onset of cellularity. For pure methanol, it is observed that the flame front becomes cellular very quickly after the ignition of a rich mixture. Adding more water into the methanol will clearly delay the onset of cellularity.

The correlated laminar burning velocity of methanol and water provides data for combustion system analysis and turbulent burning velocity estimation. The data would also be useful for validating chemical kinetic models.

Acknowledgement

None.

References

[1] Sileghem L, Alekseev VA, Vancoillie J, Nilsson EJK, Verhelst S, Konnov AA. Laminar burning velocities of primary reference fuels and simple alcohols. Fuel 2014; 115: 32–40.

[2] Brusstar, M, Stuhldreher, M, Swain, D, and Pidgeon, W, High efficiency and low emissions from a port-injected engine with neat alcohol fuels. SAE Technical Paper 2002-01-2743

[3] Pearson RJ, Turner JWG, Bell A, de Goede S, Woolard C, Davy MH, Iso-stoichiometric fuel blends: characterisation of physicochemical properties for mixtures of gasoline, ethanol, methanol and water. Proc IMechE Part D: J Automobile Engineering 2015; 229(1): 111–139

[4] Saeed K, Stone CR. Measurements of the laminar burning velocity for mixtures of methanol and air from a constant-volume vessel using a multizone model. Combust Flame 2004;139:152–66.

[5] Metghalchi M, Keck JC. Burning velocities of mixtures of air with methanol, isooctane, and indolene at high pressure and temperature. Combust Flame 1982; 48: 191–210.

[6] Gulder ÖL. Laminar burning velocities of methanol, isooctane and isooctane/methanol blends. Combust Sci Technol 2007; 33: 179–92.

[7] Liao SY, Jiang DM, Huang ZH, Shen WD, Yuan C, Cheng Q. Laminar burning velocities for mixtures of methanol and air at elevated temperatures. Energy Convers Manage 2007; 48: 857–63.

[8] Liao SY, Jiang DM, Huang ZH, Zeng K. Characterization of laminar premixed methanol–air flames. Fuel 2006; 85: 1346–53.

[9] Zhang Z, Huang Z, Wang X, Xiang J, Wang X, Miao H. Measurements of laminar burning velocities and Markstein lengths for methanol–air–nitrogen mixtures at elevated pressures and temperatures. Combust Flame 2008; 155: 358–68.

[10] Zhang Z, Huang Z, Wang X, Zheng J, Miao H, Wang X. Combustion characteristics of methanol–air and methanol–air–diluent premixed mixtures at elevated temperatures and pressures. Appl Therm Eng 2009; 29: 2680–8.

[11] Davis S, Law C. Determination of and fuel structure effects on laminar flame speeds of C1 to C8 hydrocarbons. Combust Sci Technol 1998; 140: 427–49.

[12] Egolfopoulos FN, Du DX, Law CK. A comprehensive study of methanol kinetics in freely-propagating and burner-stabilized flames, flow and static reactors, and shock tubes. Combust Sci Technol 1992; 83: 33–75.

[13] Gibbs GJ, Calcote HF. Effect of molecular structure on burning velocity. J Chem Eng Data 1959; 4: 226–37.

[14] Vancoillie J, Christensen M, Nilsson EJK, Verhelst S, Konnov AA. Temperature dependence of the laminar burning velocity of methanol flames. Energy Fuels 2012; 26: 1557–64.

[15] Sileghem L, Alekseev VA, Vancoillie J, Nilsson EJK, Verhelst S, Konnov AA. Laminar burning velocities of primary reference fuels and simple alcohols. Fuel 2014; 115: 32–40.

[16] Beeckmann J, Cai L, Pitsch H, Experimental investigation of the laminar burning velocities of methanol, ethanol, n-propanol, and n-butanol at high pressure. Fuel 2014; 117: 340–350.

[17] Katoch A, Asad A, Minaev S, Kumar S. Measurement of laminar burning velocities of methanol–air mixtures at elevated temperatures. Fuel 2016; 182: 57–63.

[18] Hinton N, Stone CR, Laminar burning velocity measurements of methane and carbon dioxide mixtures (biogas) over wide ranging temperatures and pressures. Fuel 2014; 116: 743–750.

[19] Marshall SP, Stone CR, Hegheş C, Davies TJ, Cracknell RF. High pressure laminar burning velocity measurements and modelling of methane and n-butane. Combust Theory Model 2010; 14(4): 519–40.

[20] Marshall SP, Taylor S, Stone CR, Davies TJ, Cracknell RF. Laminar burning velocity measurements of liquid fuels at elevated pressures and temperatures with combustion residuals. Combust Flame 2011; 158: 1920–32.

[21] Lewis B, Von Elbe G. Combustion, flames and explosions of gases. London, UK: Academic Press Inc.; 1961.